Received: 11 November 2020 | Accepted: 15 January 2021

DOI: 10.1111/iwj.13555

ORIGINAL ARTICLE

IWJ WILEY

Topical effect of benzalkonium bromide on wound healing and potential cellular and molecular mechanisms

Jianghe Zhang[1] | **Yan Yan**[2] | **Yujie Li**[1] | **Chengcheng Shen**[1] | **Yiming Zhang**[1]

[1]Department of Plastic and Cosmetic Surgery, Xinqiao Hospital, Army Medical University, Chongqing, China

[2]Medical Research Center, The First Affiliated Hospital of Zhengzhou University, Zhengzhou, China

Correspondence
Chengcheng Shen and Yiming Zhang, Department of Plastic and Cosmetic Surgery, Xinqiao Hospital, Army Medical University, Chongqing 400037, China.
Email: shencc2020@163.com (C. S.) and zhangyiming@tmmu.edu.cn (Y. Z.)

Funding information
National Natural Science Foundation of China, Grant/Award Number: 81971844

Abstract

Benzalkonium bromide (BB) has been widely used as a skin antiseptic for wound management. However, BB had proinflammation and reactive oxygen species (ROS) induction effect, making its role in wound healing complex and unclear. A rat full-thickness skin defect wound model was established. The effects of BB, povidone iodine (PVP-I), chlorhexidine gluconate (CHG), and normal saline (NS) on wound healing and infection control were then evaluated based on wound healing rate (WHr) and bacterial killing. The wound tissues were sectioned for histopathological evaluation and nuclear factor E2 related factor 2 (Nrf2) expression determination. The ROS production, Nrf2 activation, and heme oxygenase 1 (HO-1) expression of the HaCat cells and the cytotoxicity treated with BB were further explored. Compared with NS, PVP-I, and CHG, BB showed the best wound infection control efficiency while delayed wound healing with the WHr of 91.42 ± 5.12% at day 20. The wound tissue of the BB group showed many inflammatory cells but few granulation tissue and capillaries and no obvious collagen deposition, resulting in the lowest histopathological scores of 4.17 ± 0.75 for BB group. BB showed higher cytotoxicity on HaCat cells with the lowest IC25, IC50, and IC75 of 1.90, 4.16, and 9.09 g/mL compared with PVP-I and CHG. TUNEL staining evaluated the cytotoxicity of BB on wound tissue, which indicates the high apoptosis index BB group (5.05 ± 1.77). Compared with PVP-I and CHG, BB induced much more cell apoptosis. The results of flow cytometry and fluorescence staining showed that PVP-I, CHG, and BB induced ROS production in a concentration-dependent manner and cells treated with BB had the highest ROS production at the same inhibition concentration. The cells and the wound tissues treated with BB showed highest Nrf2 activation and HO-1 expression than PVP-I and CHG. BB was highly efficient in wound infection control while delayed wound healing. The prolonged and strengthened inflammation and the raised ROS production originating from BB administration may contribute to delayed wound healing.

KEYWORDS

benzalkonium bromide, inflammation, reactive oxygen species, wound healing, wound infection

1 | INTRODUCTION

Wound management is a common problem in clinical work and wound related complications are a major cause of mortality. Wound threaten global public health and increase medical costs worldwide.[1-3] Wound healing is a complex and dynamic physiological process that is often divided into four distinct phases: haemostasis, inflammation, proliferation, and remodelling. The complexity of wound healing makes it vulnerable to interruption. Many intrinsic and extrinsic factors, which can affect physiologic responses and cellular function can affect wound healing, including infection, blood supply, age, nutrition, and health status.[4,5] Among them, infection can delay or prevent the healing of different types of wounds.[6,7] Therefore, controlling wound infection is an effective approach to promote wound healing. Oral or topical antibiotics can effectively control wound infection. However, the microbial spectrum controlled by antibiotics is often relatively narrow. Besides, an increasing emergence of resistance to topical and systemic antibiotics has been observed. The emergence of multidrug-resistant bacteria and methicillin-resistant *Staphylococcus aureus* has reduced the efficiency of antibiotics in wound infection control. Microbial colonies in wounds often produce a biofilm, consisting of a polysaccharide extracellular matrix, to protect themselves. This can significantly reduce the bactericidal activity of antibiotics.[8,9] So, an efficient alternative strategy must be developed for wound infection control.

Antiseptics are commonly used for wound infection control and have the advantages of low cost and wide antimicrobial activity.[10] Because they kill bacteria through a variety of mechanisms, skin antiseptics rarely lead to bacterial resistance.[8] Antiseptics also provide better wound infection control because they can penetrate biofilms, necrotic tissue, and scabs. Although some antiseptics have shown poor tissue tolerance, the use of new stabilisers and carriers has greatly improved their biocompatibility and tolerance.[11] The latest World Health Organization (WHO) guidelines state that skin antiseptics should be used in preparation for surgery and antibiotics should be avoided.[12]

A variety of skin antiseptics have been used for wound infection control, including povidone iodine (PVP-I) and chlorhexidine gluconate (CHG).[13] PVP-I is an iodine-containing chemical complex that is widely used. It can slowly release free iodine to kill bacteria. Unlike the traditional iodine antiseptics, PVP-I is much less irritating. It is stable, non-cytotoxic, a non-sensitiser, and has a low potential for developing drug resistance bacteria.[10] CHG is a biguanide chlorobenzene and a cationic surfactant with strong antimicrobial effects and a broad antimicrobial spectrum. The good biocompatibility of CHG favours its use for skin disinfection, oral, and dental practice.[14,15] Although normal saline (NS) has no bactericidal effect, many studies have demonstrated that NS irrigation has an anti-infection effect on wound surfaces, making it to be an ideal candidate for wound infection control in clinical work.[16]

Benzalkonium bromide (BB) is a quaternary ammonium cationic surfactant. BB has lipophilic properties

Key Messages

- benzalkonium bromide (BB) has been widely used as skin antiseptic for wound management, while some studies have demonstrated that BB had toxic effect on mammalian cells, making its role in wound healing complex and unclear. So, we evaluated the overall effect of BB on wound healing and further explored its mechanism
- sixty male Sprague Dawley rats were used for wound healing model establishment. The effects of BB, povidone iodine (PVP-I), chlorhexidine gluconate (CHG), and normal saline (NS) on wound healing and infection control were discussed based on wound healing rate and bacterial killing. The wound tissues were sectioned for HE, Masson and TUNEL staining, and immunohistochemical staining for nuclear factor E2 related factor 2 (Nrf2) expression determination. The cytotoxicity of BB, PVP-I, CHG, and NS on HaCat cells and the reactive oxygen species (ROS) production, Nrf2 activation, and heme oxygenase 1 expression of the cells were further explored
- although BB is highly efficient in wound infection control, it shows negative overall effect on wound healing. The prolonged and strengthened inflammation and the raised ROS production may contribute to delayed wound healing

allowing it to intercalate into the lipid layer of the cell membrane, changing the ionic resistance and boosting membrane permeability or even rupturing the cell membrane. This causes leakage of the cell contents and the death of microorganisms.[17] Because of its bactericidal effect, BB has been widely used as a skin antiseptic and a preservative for eye drops. Compared with PVP-I and CHG, BB is of low bactericidal concentration and lacks an unpleasant smell. BB is colourless, making it easier to determine the wound status after BB irrigation.[18,19] However, BB may have cell toxicity because of its destructive effects on cell membrane integrity. BB can also activate excessive local inflammatory responses for cancer therapy.[20] The cytotoxicity of benzalkonium chloride (BAC), which is an analogue of BB and an eye drop preservative, has been studied. BAC has a very strong proapoptotic effect on conjunctival cells.[21] BAC can also induce the release of cytochrome C to activate caspase-9 and caspase-3 pathways, resulting in cell apoptosis. BB and BAC can produce reactive oxygen species (ROS) in cells, leading to oxidative stress on tissues and damage to normal and tumour tissues.[17,22] These findings indicate that the role of BB in wound healing is complex and unclear. Its overall effect on wound healing and its mechanism of action deserve further study.

In this study, we explored the topical effect of BB on wound healing compared with NS and other commonly used antiseptics. In addition, we further examined the potential cellular and molecular mechanisms of BB on wound tissues and HaCat cells.

2 | MATERIALS AND METHODS

2.1 | Materials

BB, PVP-I, and CHG were purchased from Lircon (Shandong, China). Masson staining solution was obtained from Jiancheng Bioengineering Institute (Nanjing, China). The In Situ Cell Death Detection Kit was purchased from Roche (Basel, Switzerland). Radio immunoprecipitation assay (RIPA) lysis buffer, protease inhibitor cocktail (for mammalian cell and tissue extracts), bicinchoninic acid (BCA) protein assay kit, and Count Kit-8 (CCK-8) was obtained from Beyotime Biotechnology Company (Beijing, China). Anti-human nuclear factor E2 related factor 2 (Nrf2) antibody (ab62352), anti-rat Nrf2 antibody (ab137550), anti-human Nrf2 (phosphoS40) antibody (ab76026), and anti-human heme oxygenase 1 (HO-1) antibody (ab68477) were all purchased from Abcam (Cambridge, United Kingdom). Actin beta (ACTB) Rabbit monoclonal antibody was obtained from Abclonal (Wuhan, China). Goat anti-Rabbit IgG (H + L) Cross-Adsorbed Secondary Antibody-Alexa Fluor 647 was purchased from Thermo Fisher Scientific (Waltham, Massachusetts). Goat anti-Rabbit diaminobenzidine (DAB) antibody was purchased from R&D systems (Minneapolis, Minnesota). Minimum essential medium (MEM) and penicillin/streptomycin were purchased from Hyclone (Logan, Utah). Foetal bovine serum (FBS) was obtained from Scitecher (Beijing, China). ROS Fluorescent indicator (H2DCFDA) was purchased from Tocris Bioscience (Bristol, United Kingdom). Phosphatidylcholine, Tween 80, and agar medium were obtained from Solarbio (Beijing, China).

2.2 | Animal model of wound healing and antiseptics treatment

Under the permission of the Animal Welfare and Ethics Committee of the Army Medical University, 60 male Sprague Dawley rats with a body weight of 200 ± 20 g were used for wound healing model establishment. The rats were purchased from Chongqing TengXin Biotechnology Co. and maintained in the experimental animal centre of the XinQiao hospital. Rats were kept at 23 ± 1°C and a relative humidity of 50 ± 10% under controlled light conditions (12:12 hours, L:D) following the 3R principle. Food and water were freely available.

After rats were anaesthetised by intraperitoneal injection of pentobarbital sodium (32.5 mg/kg body weight) and skin preparation, a circular mark (18 mm in diameter) was pressed onto the dorsal interscapular area perpendicular to the skin, and the full-thickness skin within the circular area was cut off along the indentation. After successfully modelling, the rats were divided into four groups. The control group received NS treatment, while the wounds of the other three groups were irrigated with 2 g/L BB, 0.5 g/L PVP-I, and 0.2% CHG once a day. At 6 and 9 day after treatment, five rats in each group were euthanised and their wounds were excised for histopathological and immunohistochemical assays. The wounds were photographed with a Nikon D90 camera (Tokyo, Japan) every day and then analysed with ImageJ software.

When the wounds reached epithelialisation with no moist granulation tissue and no obvious exudation, the wounds were regarded as healed. The wound closure was used for determining wound healing rate (WHr) and calculated according to the following formula (day 0 is the modelling day).

$$\text{Wound closure}(\%) = \frac{\text{Wound area on day 0} - \text{Wound area on the indicated day}}{\text{Wound area on day 0}} \times 100\%$$

2.3 | Histopathological evaluation of wound tissues

For the histopathological assay, the tissues were fixed in 4% paraformaldehyde, dehydration, transparency, waxing, embedding, sectioning, and then stained with haematoxylin-eosin. Masson staining was also performed, according to manufacturer instructions, to observe tissue collagen. Two pathologists scored the tissues based on granulation tissue, degree of epithelialisation, amount of collagen deposition, number of inflammatory cells, and angiogenesis.[23] The TUNEL method was used for the apoptosis measurement and the apoptosis index (AI) was calculated as follows:

$$\mathrm{AI}(\%) = \frac{\text{number of apoptosis cells}}{\text{total number of cells}} \times 100\%$$

For determination of Nrf2 expression, paraffin sections of wound tissue were first dewaxed. After closure with H_2O_2, the sections were incubated with rabbit anti rat Nrf2 antibody (1:250) overnight at 4°C and biotin labelled goat anti rabbit IgG for 30 minutes. After DAB chromogenic and haematoxylin staining, the tissues were observed and photographed using Olympus BX63 microscope (Olympus, Tokyo Japan).

2.4 | Bacterial killing on wound surface

Six hours after modelling, sterile swabs were used to sample the wounds before and after application of 2 g/L BB, NS, 0.5 g/L PVP-I, and 0.2% CHG. The sampled swab head was cut and placed into 5 mL HEPES (N-2-hydroxyethylpiperazine-N-2-ethanesulfonic acid) buffer containing 0.14% (wt/vol) lecithin and 1.0% (wt/vol) Tween-80, and the mixtures were rotated for 20 seconds to form a bacterial suspension. The suspensions were then diluted 10-, 100-, and 1000-fold and inoculated on a non-selective agar plate. After 48 hours incubation at 37°C, the number of colonies was counted. The killing rate (Kr) and killing logarithm value (KI) were used for the evaluation of the effect of NS, PVP-I, BB, and CHG for infection control, which was calculated as follows: Kr = (number of colonies before − number of colonies after)/number of colonies before × 100%, KI = logarithm value of colonies before − logarithm value of colonies after.

2.5 | Cell viability

Human immortalised keratinocyte HaCat cells were used for cell experiments. HaCat cells were purchased from Shanghai Cell Bank of Chinese Academy of Sciences and routinely cultured under standard conditions (humidified atmosphere of 5% CO_2 at 37°C) in complete growth medium, which was composed of 85% MEM, 15% FBS, and penicillin (100 U/mL)/streptomycin (100 g/mL). The 75% inhibitory concentration (IC75), 50% inhibitory concentration (IC50), and 25% inhibitory concentration (IC25) of BB, PVP-I, and CHG on HaCat cells were determined by the CCK-8 kit. Briefly, the HaCat cells were seeded into 96-well plates at a concentration of 10^4 /100 μL and incubated overnight for cell adherence. Then, BB, PVP-I, and CHG were diluted to corresponding concentrations with complete growth medium (0.42, 0.70, 1.17, 1.94, 3.24, 5.40, 9.00, 15.00, and 25.00 mg/L for BB; 4.75, 6.33, 8.44, 11.25, 15.00, and 20.00 mg/L for PVP-I; 1.69, 2.64, 4.12, 6.44, 10.07, 15.73, 24.58, 38.40, and 60.00 mg/L for CHG). After removing the original growth medium, 100 μL mediums with different concentrations of BB, PVP-I, and CHG were added into 96-well plates successively. After 4 hours of culturing, the medium in the 96-well plates was removed, and 100 μL of mixed medium containing 90 μL fresh complete growth medium and 10 μL WST-8 was added. After 1.5 hours of additional incubation, the absorbance of each well was measured with Thermo Scientific Varioskan LUX (Waltham, Massachusetts). The IC75, IC50, and IC25 of BB, PVP-I, and CHG were calculated using GraphPad Prism 8.

2.6 | ROS production, Nrf2 activation, and HO-1 expression analysis

For ROS analysis, HaCat cells were planted in a six-well plate. After adherence, the original medium was replaced with the medium containing BB, PVP-I, and CHG at the concentration of IC25, IC50, and IC75. After 4 hours of incubation, the medium was removed and fresh complete growth medium containing 10 μM H2DCFDA probes was added and cells were incubated for an additional 40 minutes. Cells were observed and photographed directly using the Incucyte Live cell imaging and analysis system (Ann Arbor, Michigan), and then collected for ROS detection by flow cytometry (BD Biosciences, San Jose, California). FlowJo software was used to analyse the mean fluorescence intensity (MFI).

For Nrf2 activation analysis, HaCat cells were first planted in confocal dishes overnight. Then, the cells were cultured with complete growth medium containing BB, PVP-I, and CHG at a concentration of IC25, IC50, and IC75 for 4 hours. The medium was then removed and cells were fixed, membrane penetrated, and closured in sequence. After incubation with primary antibody and secondary antibody, the cells were re-stained with 4′, 6′-diamidino-2-phenylindole (DAPI), and then observed

and photographed under a laser confocal microscope (Zeiss LSM 880; Carl Zeiss, Jena, Germany).

Nrf2 activation and HO-1 expression were analysed with western blotting. When the cells were attached to culture flask, fresh complete medium mixed with BB, PVP-I, and CHG at a concentration of IC25, IC50, and IC75 was added. After 4 hours of incubation, cells were broken for protein extraction using lysates and protease phosphatase inhibitors. The expressions of Nrf2, pNrf2, and HO-1 were determined using western blotting analysis following the procedure described previously. The cells cultured in the complete growth medium containing NS were used as the control for the ROS production, Nrf2 activation, and HO-1 expression analysis.

2.7 | Statistical analysis

A generalised linear mixed model was used to evaluate the wound healing from repeated observations. A Student's *t* test was used to compare the measurement data of two groups, and a one-way analysis of variance with Bonferroni's post hoc test was used for multiple comparisons. For non-normally distributed data, we used the Kruskal-Wallis followed by Dunn's post hoc test for statistical analysis. $P < .05$ was considered to be statistically different. All statistical work was performed using SPSS software (V20.0.0, IBM Co.).

3 | RESULTS

3.1 | Wound healing

The wounds healed and the wound area of every group decreased gradually over time. Compared with the NS group, wound healings were all delayed by different degrees after PVP-I, BB, and CHG irrigation (Figure 1A-C). Within the first 10 days, the WHr of each group were significantly different ($P < .01$). At day 20, the WHr of NS, PVP-I, BB, and CHG group reached 99.62 ± 0.54%, 92.26 ± 8.06%, 91.42 ± 5.12%, and 95.5 ± 1.95%, respectively. The generalised linear mixed model estimated that the WHr of the NS, PVP-I, BB, and CHG groups was 94.35 ± 1.13%, 82.72 ± 1.13%, 77.11 ± 1.20%, and 84.69 ± 1.13% (Figure 1C). The WHr of PVP-I, BB, and CHG group were all significantly lower than that of NS group ($P < .01$) with the estimated values of −11.63 ± 1.60, −17.25 ± 1.65, and −9.67 ± 1.60, respectively. Different from PVP-I and CHG group, which had a similar effect on wound healing ($P = .219$), BB delayed the wound healing significantly

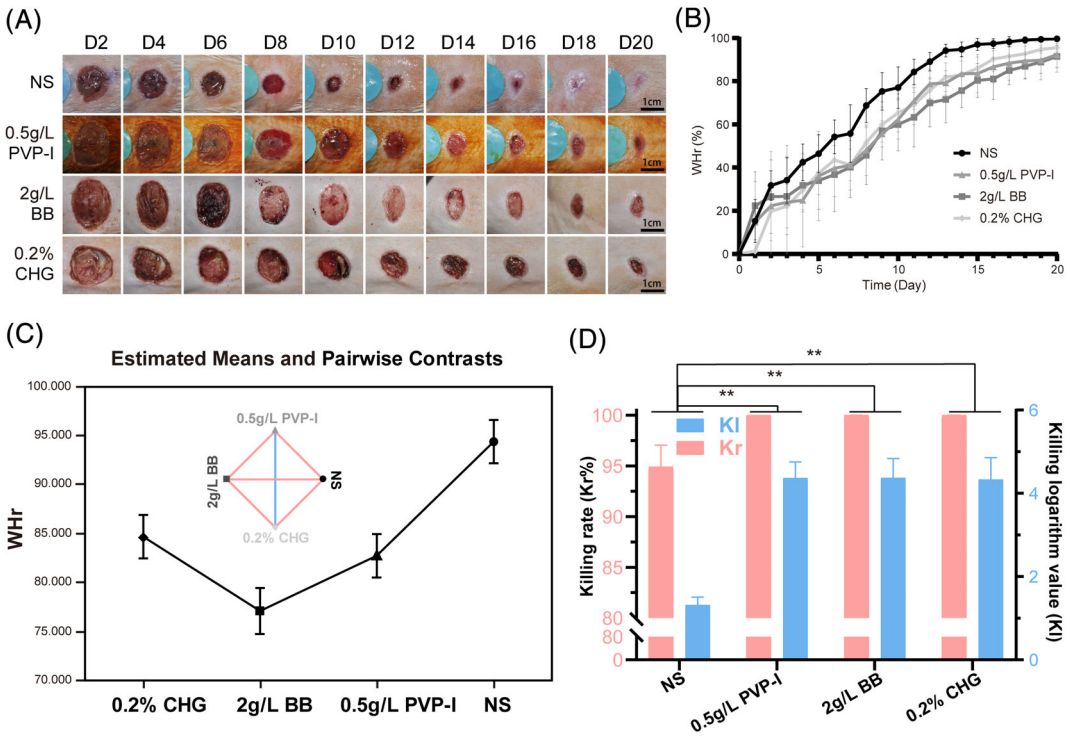

FIGURE 1 Effect of BB, PVP-I, CHG, and NS on wound healing and infection control. A, Photographs of wounds in each group. B, The wound healing rate within 20 days of BB, PVP-I, CHG, and NS treated wound. C, Estimated mean values and statistical analysis using a generalised linear mixture model (the red lines in the rhomboids indicates significant difference ($P < .05$); the blue line indicates no significant difference). D, The killing rate and killing logarithm value of BB, PVP-I, CHG, and NS (*$P < .05$; **$P < .01$)

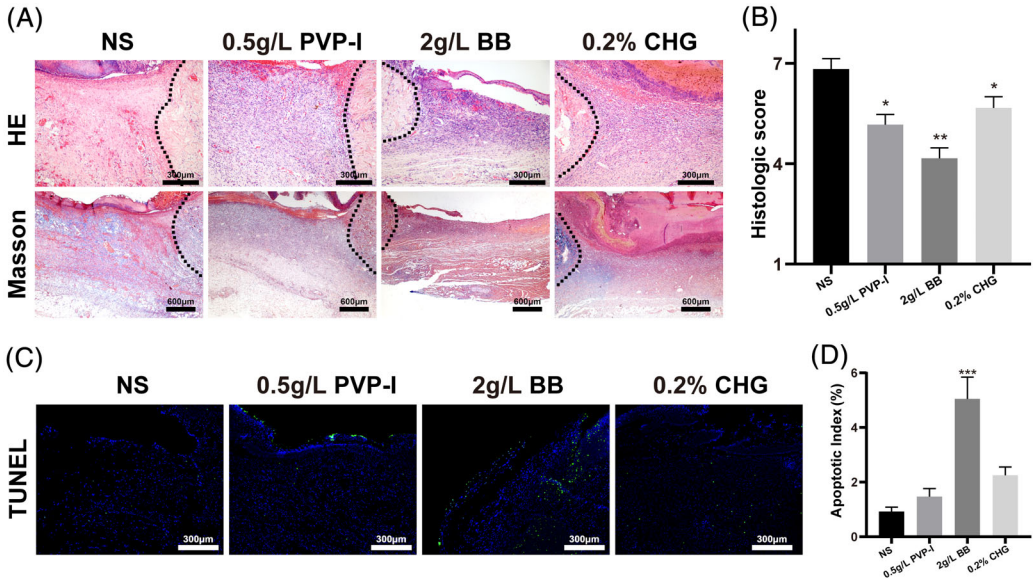

FIGURE 2 Histopathological evaluation of wound tissues. A, HE (10×) and Masson staining (4×) of wound tissues. The black dotted line is the wound edge. B, Histopathological score of wound tissues. C, The TUNEL staining of wound tissues. D, Apoptosis rate of the wound tissues in each group. ***: significant difference compared with NS group ($P < .01$)

(Figure 1C). In addition, the skin of the rats was severely corroded after irrigation with undiluted BB (30 g/L) (Figure S2).

3.2 | Histopathology

For the microscopic evaluation of wound healing and mechanism exploration, histopathological analysis of wound tissue was conducted. HE and Masson staining results are shown in Figure 2A. At day 9, inflammatory cell infiltration in the NS group had subsided. A medium thickness granulation tissue, many fibroblasts, and extensive neovascularisation were seen within the wound tissue. Many epithelial cells migrated from the margin to the centre and formed an epithelial tongue. Meanwhile, there was substantial collagen deposition within the wound. The sections of PVP-I and CHG groups were of the similar microscopic image, and contained more inflammatory cells and fewer capillaries, granulation tissue, fibroblasts, and collagen than the NS group. The wound tissue of the BB group showed a comparable number of inflammatory cells with PVP-I and CHG group, but they had much less granulation tissue and new capillaries and no obvious collagen deposition. After evaluation by two pathologists, the scores of wound tissues from the NS, CHG, PVP-I, and BB groups were 6.83 ± 0.75, 5.67 ± 0.82, 5.17 ± 0.7, and 4.17 ± 0.75, respectively. Compared with the NS group, the scores of CHG, PVP-I, and BB group were significantly lower ($P < .05$) and the tissue of the BB group received the lowest score ($P < .01$) (Figure 2B). Figure 2C shows the TUNEL staining of the wound tissues and indicates that the AI of PVP-I, CHG, and BB group (1.47 ± 0.65, 2.25 ± 0.67, and 5.05 ± 1.77) were much higher than that of the NS group (0.92 ± 0.35). Compared with PVP-I and CHG, BB induced much more cell apoptosis ($P < .01$) (Figure 2D).

3.3 | Bactericidal analysis

Figure 1D shows the KI and Kr of NS, PVP-I, CHG, and BB. The KI were 4.37 ± 0.38, 4.33 ± 0.52, and 4.37 ± 0.46 for PVP-I, CHG, and BB, which were much higher than that of NS (1.32 ± 0.19), indicating better their bactericidal effect. Although the KI of NS was significantly lower, its Kr was still more than 95%, indicating satisfactory wound infection control efficiency. There was no wound infection for all the wounds from any group during the whole wound healing process, suggesting that NS, PVP-I, CHG, and BB were all satisfactory for wound infection control (Figure 1D).

3.4 | Cytotoxicity and ROS analysis

To further explore the influence on wound healing and the possible mechanism, we evaluated cytotoxicity of NS, PVP-I, CHG, and BB on HaCat cells and quantified the intracellular ROS production of the treated cells. BB, CHG, and PVP-I had obvious concentration-dependent cytotoxicity on HaCat cells, while NS had no obvious

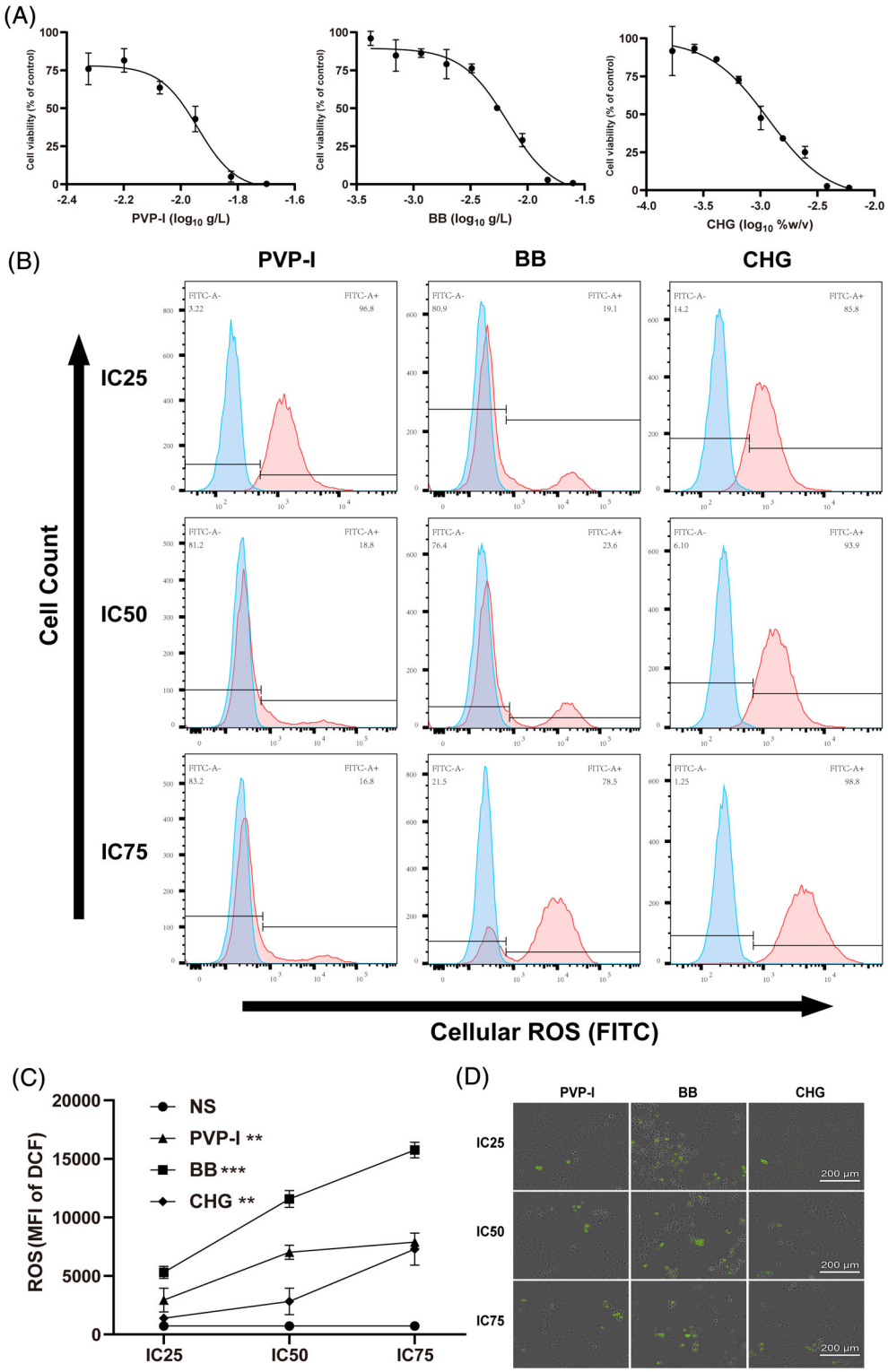

FIGURE 3 Viability and reactive oxygen species (ROS) production analysis of BB, PVP-I, CHG treated cells. A, Growth inhibition curves of cells based on CCK-8 analysis. B, ROS production of cells detected by flow cytometry. C, Mean fluorescence intensity of H2DCFDA probe in cells. D, Fluorescence images of cells after H2DCFDA probe staining. $^{**}P < .01$; $^{***}P < .001$

toxic effect. Increased treatment concentration of BB, CHG, and PVP-I decreased cell viability. Compared with PVP-I and CHG, the cells treated with BB at the same concentration showed lower viability. The IC75 of BB, CHG, and PVP-I on Hacat cells were 9.09, 19.52, and 12.13 g/mL, IC50 was 4.16, 10.01, and 8.71 g/mL, IC25 was 1.90, 5.14, and 6.26 g/mL, respectively (Figures 3A and S1).

The intracellular ROS production of cells treated with NS, PVP-I, CHG, and BB with different concentrations was quantitatively determined by flow cytometry (Figure 3B,C). PVP-I, CHG, and BB induced more ROS than NS in HaCat cells. With increasing concentration, the production of ROS increased in each group. After co-incubation with the same inhibition concentration (IC25, IC50, or IC75), cells treated with BB had the

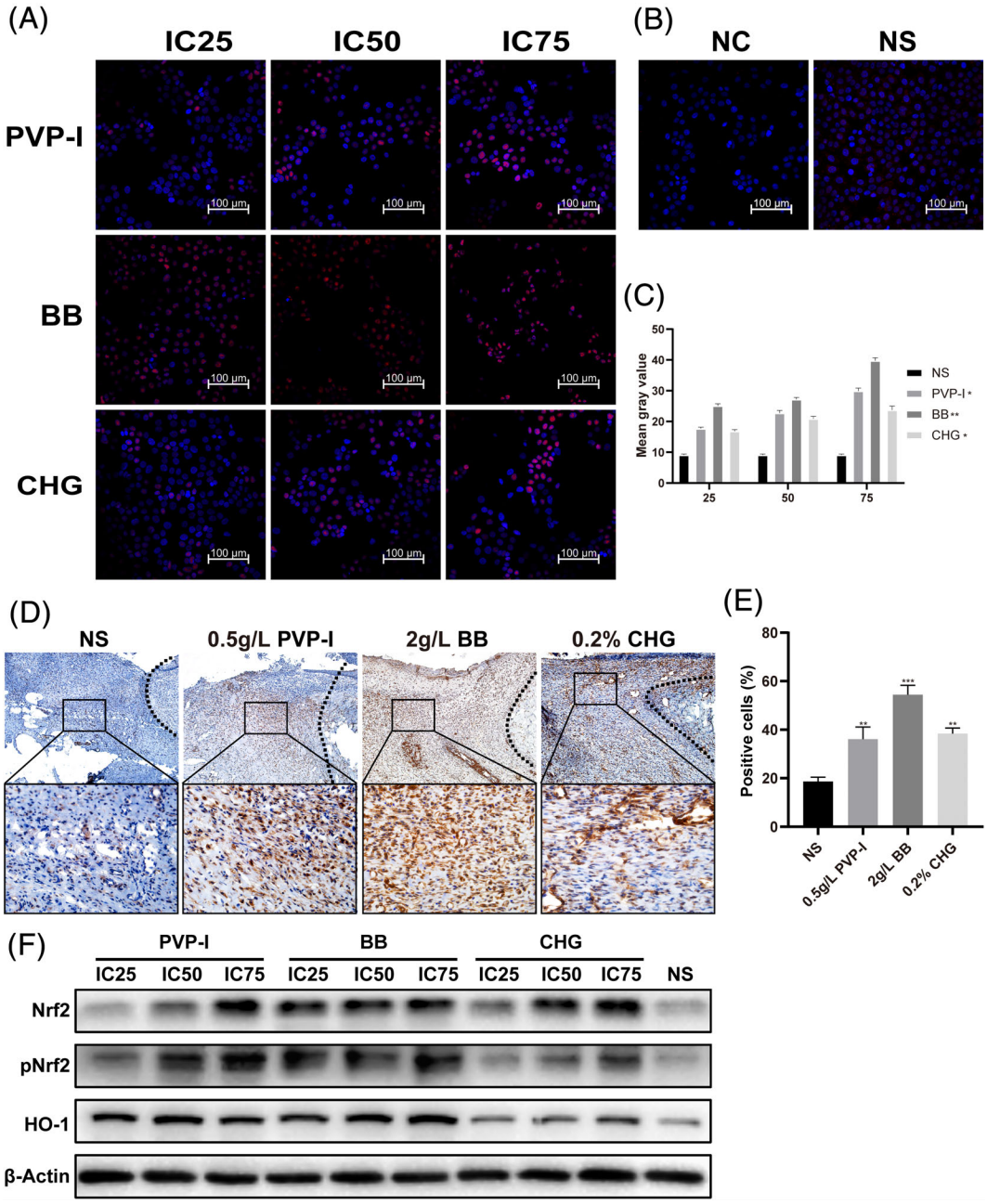

FIGURE 4 Nrf2 activation and HO-1 expression analysis. Immunofluorescent staining of activated Nrf2 in HaCat cells treated with BB, PVP-I, CHG, A, and NS and the negative control, B. C, Mean fluorescence intensity of pNrf2 in the nucleus measured using ImageJ. D, Immunohistochemical staining of Nrf2 in wound tissues. The black dotted line indicates the wound edge. E, Positive cell rate based on the Nrf2 immunohistochemical staining. F, The expressions of Nrf2, pNrf2 and HO-1 in HaCat calls determined by WB. $^{*}P < .05$; $^{**}P < .01$; $^{***}P < .001$

highest ROS production. Cells showed significant ROS induction when treated with BB concentrations as low as IC25. After treatment with a BB concentration of IC75 for 4 hours, the MFI value of ROS in HaCat cells was 15 754 ± 671.7, which was significantly higher than that of cells treated with NS, PVP-I, and CHG with a concentration of IC75 ($P < .001$). Fluorescence imaging of cells verified the quantitative analysis of ROS by the flow cytometer. PVP-I, CHG, and BB at different concentrations induced the production of ROS in cells (Figure 3D). However, cells co-incubated with BB at concentrations of IC25, IC50, or IC75 showed higher ROS production than PVP-I and CHG at the same inhibition concentration. Flow cytometry analysis and fluorescence images both showed that no significant ROS production occurred in cells treated with NS (Figure S3).

3.5 | Nrf2 activation and HO-1 expression analysis

Expression and location of Nrf2 can indirectly reflect the degree of oxidative stress in tissues and cells.[24] We evaluated the expression and activation of Nrf2 to determine the oxidative stress of wound tissues and treated cells indirectly. Figure 4A shows laser confocal microscopy images of cells treated with PVP-I, CHG, and BB at concentrations of IC25, IC50, and IC75. Nrf2 activation and translocation are present in all the cells treated with PVP-I, CHG, and BB at concentrations of IC25, IC50, and IC75. With increased concentration, more Nrf2 were activated and translocated into the nucleus of the treated cells. Compared with PVP-I and CHG, the cells incubated with BB at the same inhibition concentration had much higher Nrf2 activation (Figure 4A,C). In contrast, there was no obvious Nrf2 activation detected and the inactivated Nrf2 was located within the cytoplasm surrounding the nucleus in the NS group (Figure 4B). The cells treated with a high concentration of BB (IC75) showed morphological changes of the nucleus.

Nrf2 activation was found in rat wound tissues using immunohistochemical staining (Figure 4D). At day 6, obvious Nrf2 activation was seen in the wound tissues irrigated with PVP-I, BB, and CHG, while no Nrf2 activation was detected in the NS group. The BB irrigated wound showed a higher level of Nrf2 activation than the PVP-I and CHG irrigated wounds. Using the ImageJ software, we obtained the Nrf2 activation positive cell rates of the wound tissues treated with NS, PVP-I, BB, and CHG, which were $19.36 \pm 2.81\%$, $35.43 \pm 4.86\%$, $53.42 \pm 4.26\%$, and $37.53 \pm 3.67\%$, respectively. These data indicated that the highest Nrf2 activation was in the BB treated wound ($P < .01$) (Figure 4E).

After translocation into the nucleus, the activated Nrf2 usually binds antioxidant response elements to promote the expression of several antioxidant enzymes, including HO-1.[25] Therefore, we evaluated the expression of Nrf2, pNrf2, and HO-1 in HaCat cells treated with NS, PVP-I, CHG, and BB using western blotting to show the oxidative stress state of cells (Figure 4F). Compared with NS, all the cells treated with PVP-I, CHG, and BB at concentrations of IC25, IC50, and IC75 showed an upregulated expression of Nrf2, pNrf2, and HO-1. With increased concentration, the cells incubated with PVP-I, CHG, and BB showed greater expression of Nrf2, pNrf2, and HO-1. Compared with PVP-I and CHG, BB induced more Nrf2, pNrf2, and HO-1 expression at the same concentration.

4 | DISCUSSION

Wound healing is a complex process governed by sequential yet overlapping phases that are characterised by different biological events. Many factors influence wound healing, including ischaemia, infection, foreign bodies, oedema, and infection is one of the most important factors.[26] Local wound infection can prevent healing by prolonging and strengthening the inflammation. The microorganisms colonised within the wound can also interfere with epithelialisation, contraction, and collagen deposition. In addition, the endotoxins from bacteria will stimulate phagocytosis and the release of collagenase, resulting in the degradation and destruction of pre-existing normal collagen and tissues.[6] The local hypoxia originating from wound contamination can suppress macrophage regulated fibroblast proliferation and delay or suspend wound healing.[27] Therefore, wound infection control has been a crucial part of wound management.

Antiseptics have been used for wound treatment for centuries.[9] However, because of the toxicity of Lister's carbolic wound spray and the introduction of the antibiotic penicillin G, antiseptic use for wound infection control declined for many decades. The development of effective and well-tolerated antiseptic substances and the emergence of multidrug resistant organisms have ushered in a new era for antiseptics.[18] Many kinds of antiseptics are now used for daily clinical work, including octenidine dihydrochloride, polyhexanide, PVP-I, CHG, and quaternary ammonium compounds.[12] Although sufficient evidence is generally lacking for optimal choice of antiseptics to prevent wound infections and treat wounds, some guidelines recommend particular antiseptics for the treatment of specific wound. BB is a quaternary ammonium compound used at low bactericidal concentrations. It lacks an unpleasant smell and is clear making it desirable for wound infection control. However, some studies have demonstrated that BB can have a toxic effect on mammalian cells, making it less desirable for wound healing.[28] The application of BB for wound management is now controversial.

Antimicrobial activity is particularly desirable in antiseptics. We evaluated the wound infection control efficacy of BB using a rat wound model. Although the Kr of BB, PVP-I, and CHG were all nearly 100%, the KI of BB was slightly higher than that of PVP-I and CHG (4.373 vs 4.37 and 4.333), indicating that BB was more effective in wound infection control. However, after irrigation with BB, PVP-I, and CHG, the wound healings were all delayed compared with the NS group and the wound treated with BB had the lowest WHr of $91.42 \pm 5.12\%$ at day 20. The overall impact of BB administration was judged to be negative for wound healing.

Many coordinated biological events are involved in wound healing, including inflammation. Although inflammation is an inevitable stage of wound healing and an appropriate inflammatory response usually benefits the wound healing, prolonged, and intensified inflammation is a hallmark characteristic of delayed wound healing.[5,29] We evaluated the inflammation of the wound bed using HE staining. At day 9, inflammatory cell infiltration in NS group had subsided, while a large number of inflammatory cells were observed in the wounds treated with antiseptics, especially with BB. This phenomenon is reasonable because BB can induce IL-2, IL6, and IL-8 secretion and further activate the inflammatory response.[21] Because of the prolonged inflammation phase and failed progression into the next scheduled phase, the formation of capillaries, granulation tissue, fibroblasts, and collagen in the BB group was reduced compared with the much less NS, PVP-I, and CHG groups. Because of the pro-inflammation effect, BB has been used as a potential instillation drug for bladder cancer therapy.[20]

Excessive ROS may cause cell damage or cell death and be involved in the occurrence and development of many diseases, including diabetes, hypertension, and Alzheimer's disease.[30] BB or BAC administration can induce the production of ROS in different cells and produce cell apoptosis and necrosis.[31] ROS may also play a role in the BB related wound healing delay. In this study, cytotoxicity analysis of BB on HaCat cells showed that BB had higher cytotoxicity than PVP-I, CHG, and NS. Cells treated with BB showed the highest ROS production. High ROS levels usually produce oxidative stress in the cell. During oxidative stress, the Nrf2 expression will increase and the Nrf2 located in the cytoskeleton will separate from kelch-like ECH-associated protein 1 (Keap1). Then, the free Nrf2 will translocate into the nucleus to activate the expression of antioxidant genes and phase II detoxification enzymes, including HO-1, maintaining the intracellular oxidation-reduction homeostasis.[25,32] We further evaluated the Nrf2 activation and HO-1 expression of the treated cells and wound tissues. Fluorescence imaging of pNrf2 and western blotting of HO-1 confirmed the oxidative stress of BB treated cells indirectly. Correspondingly, The BB irrigating wound showed the highest level of Nrf2 activation. The delayed wound healing of BB probably resulted from its pro-inflammation and ROS induction effects.

5 | CONCLUSION

We evaluated the efficacy of BB on wound healing in vitro and in vivo. BB showed better KI and comparable Kr to PVP-I and CHG, indicating that BB was more effective in wound infection control. However, BB delayed wound healing and showed an overall negative effect on wound healing. The prolonged and strengthened inflammation and the raised ROS production originating from BB administration may result in the apoptosis of epidermis cells and the less formation of capillaries, granulation tissue, fibroblasts, and collagen. These effects contribute to delayed wound healing.

ACKNOWLEDGEMENTS

We thank Yiyun Qiu and L-Sun for their assistance and encouragement during the preparation of this manuscript.

CONFLICT OF INTEREST

The authors declare no conflict of financial interest or benefit.

DATA AVAILABILITY STATEMENT

The article file contains all the datasets that support the conclusions of this study.

REFERENCES

1. Kandhwal M, Behl T, Kumar A, Arora S. Understanding the potential role and delivery approaches of nitric oxide in the chronic wound healing management. *Curr Pharm Des*. 2020;26.
2. Sorg H, Tilkorn DJ, Hager S, Hauser J, Mirastschijski U. Skin wound healing: an update on the current knowledge and concepts. *Eur Surg Res*. 2017;58(1–2):81-94.
3. Powers JG, Higham C, Broussard K, Phillips TJ. Wound healing and treating wounds chronic wound care and management. *J Am Acad Dermatol*. 2016;74(4):607-625.
4. Diegelmann RF, Evans MC. Wound healing: an overview of acute, fibrotic and delayed healing. *Front Biosci*. 2004;9:283-289.
5. Broughton G 2nd, Janis JE, Attinger CE. Wound healing: an overview. *Plast Reconstr Surg*. 2006;117(7 Suppl):1e-S-32e-S.
6. Ryan TJ. Infection following soft tissue injury: its role in wound healing. *Curr Opin Infect Dis*. 2007;20(2):124-128.
7. Rutala WA, Weber DJ. Disinfection, sterilization, and antisepsis: an overview. *Am J Infect Control*. 2019;47:A3-A9.
8. Barreto R, Barrois B, Lambert J, Malhotra-Kumar S, Santos-Fernandes V, Monstrey S. Addressing the challenges in antisepsis: focus on povidone iodine. *Int J Antimicrob Agents*. 2020;56(3):106064.
9. White RJ, Cooper R, Kingsley A. Wound colonization and infection: the role of topical antimicrobials. *Br J Nurs*. 2001;10(9):563-578.
10. Selvaggi G, Monstrey S, Van Landuyt K, Hamdi M, Blondeel P. The role of iodine in antisepsis and wound management: a reappraisal. *Acta Chir Belg*. 2003;103(3):241-247.
11. Eberlein T, Assadian O. Clinical use of polihexanide on acute and chronic wounds for antisepsis and decontamination. *Skin Pharmacol Physiol*. 2010;23:45-51.
12. Boyce JM. Best products for skin antisepsis. *Am J Infect Control*. 2019;47:A17-A22.

13. Privitera GP, Costa AL, Brusaferro S, et al. Skin antisepsis with chlorhexidine versus iodine for the prevention of surgical site infection: a systematic review and meta-analysis. *Am J Infect Control*. 2017;45(2):180-189.
14. da Silveira Teixeira D, de Figueiredo MAZ, Cherubini K, de Oliveira SD, Salum FG. The topical effect of chlorhexidine and povidone-iodine in the repair of oral wounds. A Rreview. *Stomatologija*. 2019;21(2):35-41.
15. Ritter B, Herlyn PKE, Mittlmeier T, Herlyn A. Preoperative skin antisepsis using chlorhexidine may reduce surgical wound infections in lower limb trauma surgery when compared to povidone-iodine—a prospective randomized trial. *Am J Infect Control*. 2020;48(2):167-172.
16. Owens BD, White DW, Wenke JC. Comparison of irrigation solutions and devices in a contaminated musculoskeletal wound survival model. *J Bone Joint Surg*. 2009;91A(1):92-98.
17. Debbasch C, Brignole F, Pisella PJ, Warnet JM, Rat P, Baudouin C. Quaternary ammoniums and other preservatives' contribution in oxidative stress and apoptosis on Chang conjunctival cells. *Invest Ophthalmol Vis Sci*. 2001;42(3):642-652.
18. Kramer A, Dissemond J, Kim S, et al. Consensus on wound antisepsis: update 2018. *Skin Pharmacol Physiol*. 2018;31(1):28-58.
19. Choi SM, Roh TH, Lim DS, Kacew S, Kim HS, Lee B-M. Risk assessment of benzalkonium chloride in cosmetic products. *J Toxicol Environ Health B Crit Rev*. 2018;21(1):8-23.
20. Xu R, Zhang L, Zhao X, et al. Benzalkonium bromide as a new potential instillation drug for bladder cancer: hypothesis and pilot study. *Med Sci Monit*. 2011;17(12):HY36-HY39.
21. Kwon D, Lim Y-M, Kwon J-T, et al. Evaluation of pulmonary toxicity of benzalkonium chloride and triethylene glycol mixtures using in vitro and in vivo systems. *Environ Toxicol*. 2019;34(5):561-572.
22. Cha SH, Lee JS, Oum BS, Kim CD. Corneal epithelial cellular dysfunction from benzalkonium chloride (BAC) in vitro. *Clin Experiment Ophthalmol*. 2004;32(2):180-184.
23. Greenhalgh DG, Sprugel KH, Murray MJ, Ross R. PDGF and FGF stimulate wound healing in the genetically diabetic mouse. *Am J Pathol*. 1990;136(6):1235-1246.
24. Shaw P, Chattopadhyay A. Nrf2-ARE signaling in cellular protection: mechanism of action and the regulatory mechanisms. *J Cell Physiol*. 2020;235(4):3119-3130.
25. Bellezza I, Giambanco I, Minelli A, Donato R. Nrf2-Keap1 signaling in oxidative and reductive stress. *BBA-Mol Cell Res*. 2018;1865(5):721-733.
26. Velnar T, Bailey T, Smrkoli V. The wound healing process: an overview of the cellular and molecular mechanisms. *J Int Med Res*. 2009;37(5):1528-1542.
27. Rodriguez PG, Felix FN, Woodley DT, Shim EK. The role of oxygen in wound healing: a review of the literature. *Dermatol Surg*. 2008;34(9):1159-1169.
28. Jeon H, Kim D, Yoo J, Kwon S. Effects of benzalkonium chloride on cell viability, inflammatory response, and oxidative stress of human alveolar epithelial cells cultured in a dynamic culture condition. *Toxicol in Vitro*. 2019;59:221-227.
29. Bigliardi PL, Alsagoff SAL, El-Kafrawi HY, Pyon J-K, Wa CTC, Villa MA. Povidone iodine in wound healing: a review of current concepts and practices. *Int J Surg*. 2017;44:260-268.
30. Droege W. Free radicals in the physiological control of cell function. *Physiol Rev*. 2002;82(1):47-95.
31. Tsai T-Y, Chen T-C, Wang IJ, et al. The effect of resveratrol on protecting corneal epithelial cells from cytotoxicity caused by moxifloxacin and benzalkonium chloride. *Invest Ophthalmol Vis Sci*. 2015;56(3):1575-1584.
32. Shen CC, Chen B, Gu JT, et al. The angiogenic related functions of bone marrow mesenchymal stem cells are promoted by CBDL rat serum via the Akt/Nrf2 pathway. *Exp Cell Res*. 2016;344(1):86-94.

SUPPORTING INFORMATION

Additional supporting information may be found online in the Supporting Information section at the end of this article.

How to cite this article: Zhang J, Yan Y, Li Y, Shen C, Zhang Y. Topical effect of benzalkonium bromide on wound healing and potential cellular and molecular mechanisms. *Int Wound J*. 2021;18:566–576. https://doi.org/10.1111/iwj.13555